Clinical Neurophysiology 122 (2011) 2100–2109

Contents lists available at ScienceDirect

Clinical Neurophysiology

journal homepage: www.elsevier.com/locate/clinph

A novel approach for computer assisted EEG monitoring in the adult ICU

Marleen C. Cloostermans *, Cecile C. de Vos, Michel J.A.M. van Putten

Department of Neurology and Clinical Neurophysiology, Medisch Spectrum Twente, Enschede, The Netherlands
MIRA – Institute for Biomedical Technology and Technical Medicine, Twente University, Enschede, The Netherlands

See Editorial, pages 1901–1903

ARTICLE INFO

Article history:
Accepted 17 February 2011
Available online 6 April 2011

Keywords:
Continuous EEG monitoring
Intensive care unit
Computer interpretation
Seizures
Ischemia

HIGHLIGHTS

- We present a novel computer assisted EEG interpretation system, based on a combination of eight quantitative features, to be used during EEG monitoring in the adult ICU.
- Our system provides an initial, reasonably accurate interpretation (85%) of the most common EEG patterns observed in neurological ICU patients.
- Computer assisted EEG monitoring may improve early detection of seizure activity and ischemia in critically ill patients.

ABSTRACT

Objective: The implementation of a computer assisted system for real-time classification of the electroencephalogram (EEG) in critically ill patients.
Methods: Eight quantitative features were extracted from the raw EEG and combined into a single classifier. The system was trained with 41 EEG recordings and subsequently evaluated using an additional 20 recordings. Through visual analysis, each recording was assigned to one of the following categories: normal, iso-electric, low voltage, burst suppression, slowing, and EEGs with generalized periodic discharges or seizure activity.
Results: 36 (88%) recordings from the training set and 17 (85%) recordings from the test set were classified correctly. A user interface was developed to present both trend-curves and a diagnostic output in text form. Implementation in a dedicated EEG monitor allowed real-time analysis in the intensive care unit (ICU) during pilot measurements in four patients.
Conclusions: We present the first results from a computer assisted EEG interpretation system, based on a combination of eight quantitative features. Our system provided an initial, reasonably accurate interpretation by non-experts of the most common EEG patterns observed in neurological patients in the adult ICU.
Significance: Computer assisted EEG monitoring may improve early detection of seizure activity and ischemia in critically ill patients.

1. Introduction

Evaluation of the brain function in patients from the intensive care unit (ICU) is important, since these patients are at risk of several secondary brain injuries such as (non-convulsive) seizures, cerebral ischemia and increased cerebral pressure (Claassen et al., 2005; Friedman et al., 2009). Clinical examination of these critically ill patients is however limited, even more so when they are sedated and ventilated (Jordan, 1999; Scheuer, 2002; Friedman et al., 2009). Monitoring of the brain in these patients is therefore highly desirable. Neuroimaging provides good anatomical information, but its functional information is very often limited and typically of a discontinuous nature (Tempelhoff and Yoder, 2008; Friedman et al., 2009). Since the electroencephalogram (EEG) is sensitive to changes in brain activity caused by both epileptic

* Corresponding author at: Department of Neurology and Clinical Neurophysiology, Medisch Spectrum Twente, Enschede, The Netherlands. Tel.: +31 53 4895310; fax: +31 53 4893288.
E-mail address: m.c.cloostermans@tnw.utwente.nl (M.C. Cloostermans).

1388-2457/$36.00
doi:10.1016/j.clinph.2011.02.035

seizures and ischemia, continuous EEG (cEEG) can provide a useful tool for real-time brain monitoring (Scheuer, 2002; Hirsch and Kull, 2004; Jordan, 2004; Claassen et al., 2005; van Putten, 2005; Oddo et al., 2009; Friedman et al., 2009). Among others, Jordan evaluated the usefulness and clinical impact of cEEG monitoring in the neuroscience ICU. They concluded that 86% of all cEEG recordings in the neuroscience ICU had an impact on clinical management (Jordan, 1995).

Despite the potential clinical relevance of cEEG monitoring in the ICU, its use in many ICUs remains limited. One of the main reasons for this involves the complex and time-consuming task of interpretation of each recording by means of visual analysis (Claassen et al., 2005; van Putten, 2005; Tempelhoff and Yoder, 2008). Raw EEG can hardly be interpreted by non-experts, which includes most ICU nurses and ICU physicians. To overcome this problem, several attempts have been made in computer-assisted real-time detection of deteriorations in brain function by extracting quantitative EEG (qEEG) features from the raw data. Such systems make earlier diagnostics and treatment possible. For example, various qEEG features have been proposed to detect seizures (Gotman et al., 1997; van Putten et al., 2005; Slooter et al., 2006; Deburchgraeve et al., 2008), to identify vasospasms after subarachnoid hemorrhage (Vespa et al., 1997; Claassen et al., 2004a), to differentiate between patients with good neurologic outcomes and those with poor outcomes after cardiac arrest (Jia et al., 2008; Wennervirta et al., 2009), and to predict the clinical outcome of (sub-) acute stroke patients (Finnigan et al., 2004; Finnigan et al., 2007; Sheorajpanday et al., 2009). However, these features have only focused on specific patient categories.

Ideally, all feature types should be combined into one overall system capable of classifying the common EEG patterns observed in the ICU with reasonable accuracy. This will allow unambiguous interpretation of the EEG by ICU personnel. The patterns to detect in the adult ICU should include normal EEGs, iso-electric EEGs, low voltage EEGs, burst suppression patterns, EEGs with regional or diffuse slowing (e.g. due to ischemia in post-anoxic and stroke patients, contusions in trauma patients or postictal slowing), EEGs with seizure activity, and EEGs with generalized periodic discharges (GPDs). In addition, an adequate representation of the information is required, providing relevant information to ICU personnel in a simple and clear manner, while presenting a more detailed analysis (including raw EEG data) to the consulting neurologist or clinical neurophysiologist.

This paper describes the implementation of a real-time EEG classification system based on a combination of several qEEG features. The creation of such a system is a first step towards real-time, computer-assisted detection of deteriorations in brain function, including seizure activity and ischemia in critically ill patients.

2. Methods

2.1. Patient data

EEG data for training and evaluation was selected from the digital EEG database of the Medisch Spectrum Twente hospital. All EEG registrations in the database were classified by experienced electroencephalographers using standard visual analysis. Both training and test set contained a representative set of EEG patterns. At least one 5 min epoch was selected in each EEG, reviewed by an experienced electroencephalographer (MvP) for a second time, and assigned to one of the above described categories. Uniform epochs were used so that each of them contained only a single EEG pattern. In addition, only epochs with minimal or no artefacts were used (as judged from visual inspection) with the exception of three. These three epochs contained many artefacts and were used for an initial training step to detect artefacts. The epoch selection and second review by the electroencephalographer was done prior to the automated epoch classification by our system. Therefore, the classification by the electroencephalographer was blinded to the output of the system.

All EEGs were recorded with 19 electrodes placed on the scalp according to the 10–20 system. The impedances were kept below 5 kOhm to reduce polarization effects and the sampling frequency was either 250 Hz or 256 Hz. All recordings were made using a BrainLab EEG recording system (OSG BVBA, Belgium) or Neurocenter EEG (Clinical Science Systems, Leiden, Netherlands). The Institutional Review Board waived the need for medical ethical assessment and informed consent, since all recordings were performed as a standard procedure in the clinical evaluation of the patients.

2.1.1. Training set

The training set consisted of 41 EEG epochs with a duration of 5 min each, recorded from 39 different patients. Thirty-five of these patients were admitted in the ICU, three were healthy outpatients with normal EEGs and one patient was admitted to the stroke unit. To train the system for artefact detection, three epochs were included that contained a considerable amount of artefacts.

2.1.2. Test set

An independent test set, containing epochs from different patients than included in the training set, was used for the evaluation. Seventeen of these recordings were from ICU patients and three were from outpatients. All selected epochs contained artefact free, 5 min duration EEG data. To prevent a selection bias, the test set was selected from the EEG database by a physician who was naive for the current study. Details of the training and test set are summarized in Tables 1 and 2.

2.1.3. Evaluation in the ICU

Real-time pilot measurements were performed in four ICU patients to evaluate the technical feasibility of the classifier during real-time EEG registrations.

2.2. Feature extraction

The implementation of the system was divided into several steps. First, all signals were filtered by a zero-phase 6th order butterworth bandpass filter (from 0.5 to 30 Hz) and transformed to both source and longitudinal bipolar montages. Subsequently, eight qEEG features were calculated. Based on these features, a classification was made for every 10 s segment by using a decision tree. Finally, a single interpretation for each 5 min epoch was determined. All routines were implemented in Matlab (The Mathworks Inc.).

A set of features was calculated for each 10 s segment of EEG. Most features, except for the Brain Symmetry Index (BSI) and burst and suppression index were calculated after re-referencing the EEG to the source montage. To limit the potential contribution of eye blink artefacts, the two most frontal channels Fp1 and Fp2 were discarded for these feature types. To calculate the burst and suppression index, all 19 channels (including Fp1 and Fp2) were used. The longitudinal bipolar derivations F4–C4, C4–P4, P4–O2, F3–C3, C3–P3, P3–O1, F8–T4, T4–T6, T6–O2, F7–T3, T3–T5, and T5–O1 were used to calculate the BSI. For both the burst and suppression index and the BSI, a single value was obtained for the complete 10 s EEG epoch. This is in contrast with the rest of the features, which provided a value for each individual channel separately.

For the features based on the power spectrum, a power spectral density was estimated using Welch's averaged periodogram method. Each 10 s segment of EEG was windowed for each channel and detrended using a Hamming window with a length of 512 sample

Table 1
Results of the training set. In column 3, 'c' and 'x' denotes correctly and incorrectly classified epochs respectively. BS = burst suppression pattern, DS = diffuse slowing, RS = regional slowing, GPDs = generalized periodic discharges, PAE = post-anoxic encephalopathy.

Patient #	EEG pattern	Results	Remarks
1–4	Normal	c	One ICU patient and three outpatients
5–7	Iso-electric	c	Two EEGs had ECG artefacts
8	Low voltage	c	
9	BS (with several types of artefacts)	x	Suppressions were missed because of the artefacts. A correct warning about artefacts was given
10a	BS (bursts contains EMG activity)	c	Interpreted as high frequency artefacts
10b	Same EEG as 10a, but after an injection with a muscle relaxant (Esmeron)	c	Interpreted as a burst suppression pattern
11–13	BS	c	
14	BS	x	Interpreted as slowing, because most (low amplitude) bursts were missed
15–16	DS in a patient with PAE	c	
17a	DS + RS in a neurotrauma patient	c	
17b	Same EEG as no. 17a, but a few hours later after further deterioration	c	
18–22	DS + RS in a neurotrauma patient	c	
23	DS in a neurotrauma patient	x	One brain region was interpreted as seizure activity instead of slowing
24	RS in a neurotrauma patient	c	
25–26	DS + RS in a post-surgical patient	c	
27	DS + RS in a stroke patient	c	Measured in the stroke unit
28	DS + RS in a coma patient.	c	
29	DS + GPDs in a patient with PAE	x	(Low amplitude) GPDs were missed, the DS was classified correct
30	GPDs in a neurosurgery patient	c	
31–34	GPDs	c	
35–36	Non-convulsive status epilepticus.	c	
37–38	DS + EMG artefacts	c	
39	DS + high amplitude artefacts	x	Artefacts were interpreted as seizure activity

Table 2
Results of the test set. In column 3, 'c' and 'x' denotes correctly and incorrectly classified epochs respectively. BS = burst suppression pattern, DS = diffuse slowing, RS = regional slowing, GPDs = generalized periodic discharges, PAE = post-anoxic encephalopathy.

Patient #	EEG pattern	Results	Remarks
1–2	Normal EEG	c	Measured in outpatients
3–4	Iso-electric	c	
5	Low voltage EEG, but normal EEG	x	ECG artefacts were interpreted as bursts
6	Low voltage EEG, but normal EEG	x	Measured in an outpatient. Most epochs were interpreted as normal and not as low voltage
7–10	BS	c	Two with long (>20 s) and two with short (<10 s) interburst intervals
11–12	DS in a patient with PAE	c	
13–14	DS + RS in a neurotrauma patient	c	
15	DS + RS in a coma patient	c	
16	DS + RS in a surgical patient	c	
17	DS + GPDs	x	GPDs were missed, the DS was classified correct
18	GPDs	c	
19	Seizure activity and/or GPDs	c	
20	Non-convulsive status epilepticus	c	

points. The resulting spectra from each segment were averaged and one spectral density with a resolution of approximately 0.5 Hz was obtained per channel.

2.2.1. Mean amplitude

The mean amplitude of the EEG was primarily used to classify iso-electric EEGs and low voltage EEGs. In addition, signals with very high mean amplitudes were interpreted as containing either seizure activity or artefacts, depending on the outcome of the other features. The mean amplitude of each channel was calculated as the mean of the absolute value of that channel.

2.2.2. Frequency analyses

The alpha to delta ratio (ADR) (Claassen et al., 2004a; Finnigan et al., 2007; Leon-Carrion et al., 2009) and spectral edge frequency (SEF_x) (Tonner and Bein, 2006) were used to detect slowing of the EEG patterns. The ADR is calculated as the power ratio between the alpha (8–13 Hz) and delta band (0.5–4 Hz). The SEF_x is the frequency below which a certain percentage (denoted by x) of the total power is located. In this study, the SEF_{90} was used and the total power was defined as the power between 0.5 and 15 Hz. To detect high frequency artefacts such as those caused by muscle contractions, we introduced a 'high to low frequency power ratio': the power ratio between 25–30 and 0.5–25 Hz.

2.2.3. Burst and suppression index

For the detection of burst suppression patterns and GPDs, a novel burst and suppression index was introduced as illustrated in Fig. 1. First, the signal was pre-processed with a non-linear energy operator (NLEO), defined as

$$\phi(n) = |(x_{n-1} \cdot x_{n-2}) - (x_n \cdot x_{n-3})|, \quad (1)$$

where x_n denotes the current sample of signal x, x_{n-1} the first sample before sample n, etc. (Deburchgraeve et al., 2008). This pre-processed signal shows which parts of the EEG have a high local energy (high amplitude and/or high frequency). A moving threshold was used to detect the energy increases in the signal. The running threshold was set at four times the mean plus four times the standard deviation of the preceding 0.5 s of the signal, with a minimum of 10 μV^2. After the detection of a burst, the 0.5 s that followed were

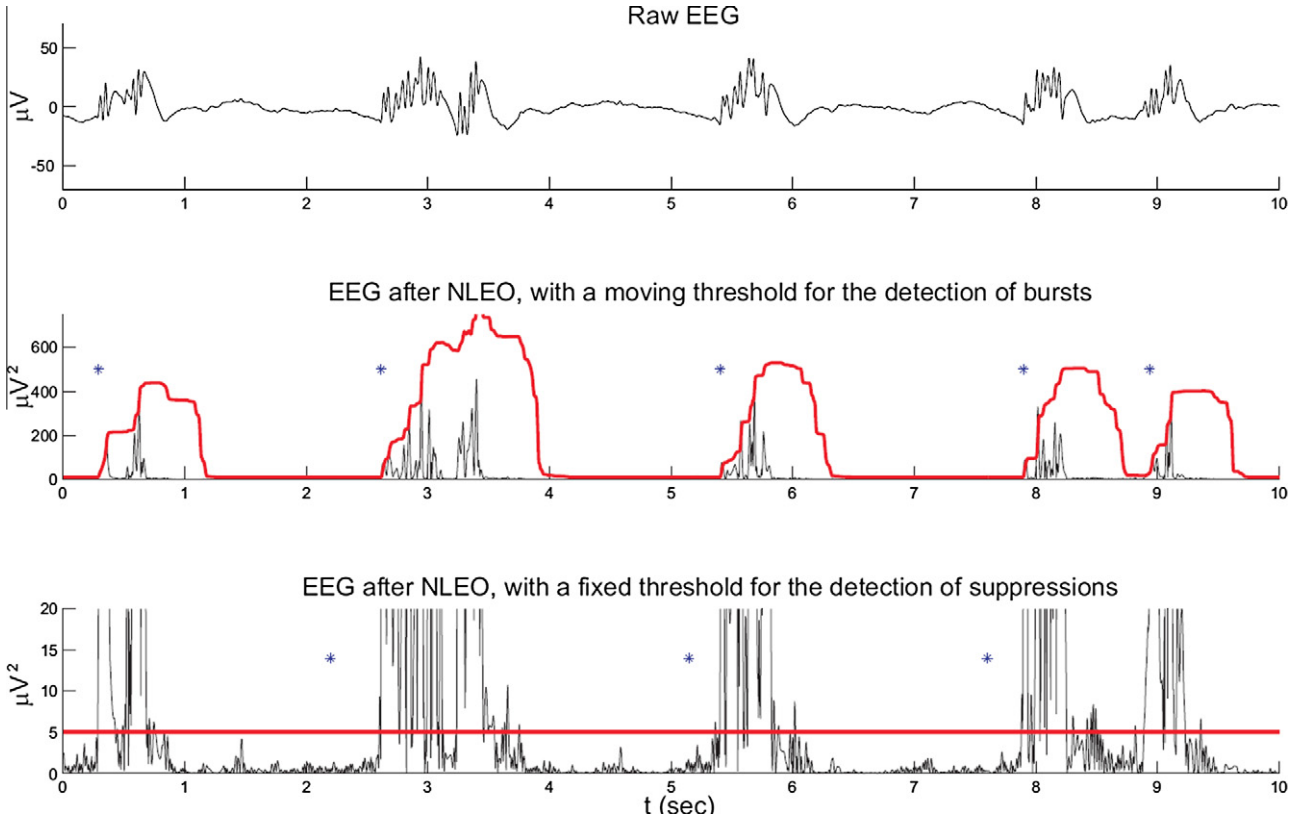

Fig. 1. Burst and suppression index for one channel. The raw EEG is shown in the upper plot and the middle plot shows the same EEG after applying a NLEO (black) together with a running threshold (red) for the detection of bursts. The threshold is based on the mean and standard deviation of the previous 0.5 s of the signal. The detected bursts are marked with blue asterisks. The bottom plot shows the same EEG after the NLEO was applied, but the *y*-axis is scaled. The thick red line in this figure represents the fixed threshold for the detection of suppressions. A suppression is detected (marked with a blue asterisk) if the signal is below this threshold for more than 1.5 s. (For interpretation of the references in color in this figure legend, the reader is referred to the web version of this article.)

ignored to prevent a single burst from being detected more than once. This was performed for all 19 channels. A burst was required to be present in more than 10 channels simultaneously (within a window of 0.2 s) to be classified as a true burst. Suppressions were detected in a comparable way. The same NLEO was applied to the EEG, but the threshold for the detection of suppressions was fixed at 5 μV^2. If the amplitude of the signal was below this value for more than 1.5 s in 10 or more channels at the same time, it was interpreted as a suppression. A 10 s epoch of EEG was interpreted as a burst suppression pattern if at least one burst and one suppression were detected in that epoch. GPDs were detected with the same method as the burst detection method. Generally, GPDs occur multiple times in a 10 s epoch. Therefore, 10 s of EEG with three or more bursts and without any suppressions were interpreted as GPDs.

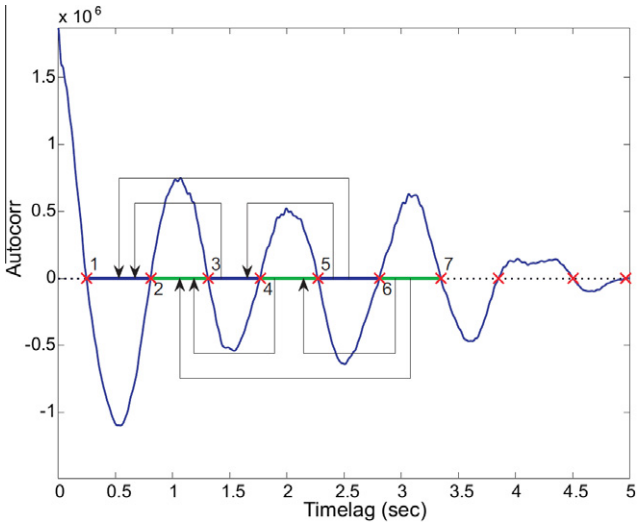

Fig. 2. Autocorrelation of an EEG epoch with seizure activity. Intervals between the zero-crossings of this autocorrelation are regular. The arrows indicate which intervals are compared (each interval is used twice).

2.2.4. Nearest neighbor coherence

The nearest neighbor synchronization is the coherence between a particular electrode and its surrounding (nearest neighbor) electrodes (van Putten, 2005). Since synchronization is often increased during seizure activity, this feature was chosen as one of the features for the detection of seizures. The nearest neighbor coherence was implemented as the mean coherence between each channel and its neighbors in the frequency range between 0.5 and 15 Hz.

2.2.5. Periodicity based on autocorrelation analysis

The periodicity of the EEG is often increased during seizures as well. To detect epochs with an increased periodicity, a measure for periodicity was used based on autocorrelation. This was done similar to the method proposed by Liu et al. (1992) and Deburchgraeve et al. (2008)). First, the autocorrelation functions for each window of 5 s were calculated with an overlap of 4 s. This was done for all channels. The zero-crossings in these autocorrelation functions were then detected. To be classified as true zero-crossings, the maximum autocorrelation value and the time interval between two zero-crossings had to be larger than a given threshold. After

detecting the zero-crossings, the ratios between different zero-crossing intervals were calculated. An example of this is shown in Fig. 2. The mean value of these ratios was used as a measure for the periodicity. The value approaches 1 for signals with high periodicity and becomes higher or lower than 1 for signals without periodicity. If less than four or more than sixty zero-crossings were present, the signal was considered as non-periodic, and the measure of periodicity was not calculated. Also, epochs with very low energy (mean value of a signal of less than 2 μV^2 after applying NLEO) were ignored. The measure for periodicity was calculated for each channel and for each 5 s window. The measures for each window in a single epoch were averaged per channel and the ignored epochs were discarded. This resulted in a single value per channel per epoch. In some cases, all windows of a channel were ignored in the calculation. These channels were then interpreted as non-periodic.

2.2.6. Brain Symmetry Index

The Brain Symmetry Index (BSI) was designed to detect asymmetries between the left- and right hemispheres of the brain (van Putten and Tavy, 2004; van Putten, 2006; van Putten, 2007). In this study, we used a pair-wise derived variant of the BSI comparable to the variant recently introduced by Sheorajpanday et al. (2009). For this variant, the BSI is defined as

$$\mathrm{BSI}(t) = \frac{1}{MK}\sum_{ch=1}^{M}\sum_{n=1}^{K}\left|\frac{R_{n,ch}(t) - L_{n,ch}(t)}{R_{n,ch}(t) + L_{n,ch}(t)}\right|, \quad (2)$$

with $R_{n,ch}(t) = a^2_{n,ch}(t)$ for channels in the right hemisphere, and a similar expression for channels in the left hemisphere. Here, K is the number of Fourier coefficients and M is the number of channel pairs, while $a_{n,ch}(t)$ denotes the Fourier coefficient with index n of channel ch evaluated at time t. Hereby, t corresponds to a particular epoch $[t - T, t]$ with duration T. A period of 10 s was used for T and the BSI was calculated in the frequency range from 0.5 to 25 Hz with a spectral bandwidth of 0.5 Hz. The BSI is bounded in range between zero (perfect symmetry for all channels) and 1 (maximum asymmetry). The pairwise variant of the BSI was used to increase the sensitivity for abnormalities that affect different regions in both hemispheres (for example patients with traumatic brain injury). In contrast to the study of Sheorajpanday et al., we used a bipolar longitudinal montage in the calculation of the pair-wise derived variant of the BSI.

2.3. Classification: decision tree

To preserve relevant information about localization and time, our system classified each 10 s epoch in four defined brain regions: left anterior, left posterior, right anterior and right posterior. The left anterior region consisted of channels F8, F4, Fz, T4, C4 and Cz, the left posterior region T3, C3, Cz, T5, P3, Pz and O1, the right anterior region F7, F3, Fz, T3, C3 and Cz, and the right posterior region T4, C4, Cz, T6, P4, Pz and O2. To obtain a classification per region, the feature values of all channels in that region were averaged and used in the decision tree. Since the periodicity measure did not necessarily have a value for each channel, the third lowest value of all non-discarded channels in each brain region was used.

A decision tree was constructed based on the prior knowledge about EEG patterns in several conditions as encountered in ICU patients. In this way, we tried to mimic the way a neurologist would describe the EEG. After the initial design, the decision tree was improved by using EEG recordings from the training set. In several steps, the boundary values and the order of the features were adapted to improve the outcome of the classified training set. For each step, we analyzed which EEG patterns were classified incorrectly and for what reason. Focus was not only placed on the percentage of falsely classified patterns, but we also considered the severity of a misclassification in clinical practice. For example, the detection of patterns with seizure activity and slowing was implemented with a cut-off value which had a relatively high sensitivity (and lower specificity), while it was decided to be more conservative with the definition of an iso-electric EEG by limiting the sensitivity for that category. Table 3 shows which features were eventually used to classify each pattern. The final version of the decision tree was applied on the training set again, and afterwards on the independent test set.

In general, the most discriminating features should appear first in the decision tree (Russell and Norvig, 1995). For our system, the mean amplitude was the most discriminating feature; EEGs with very low mean amplitudes can only be iso-electric or low-voltage and almost all other features cannot be defined reliably. Similarly, EEGs with high mean amplitudes typically contain burst suppression patterns, seizure activity or (high amplitude) artefacts. The mean amplitude was therefore the first feature evaluated in the tree. Subsequently, EEG epochs with an increased 'high to low frequency power ratio' were classified as epochs with artefacts, since further classification of signals with many artefacts is unreliable. Then, the presence of bursts and suppressions was evaluated to detect burst suppression patterns and GPDs. If the signal did not contain any bursts, the EEG was tested for seizure activity by evaluating the synchronization, periodicity and amplitude. The seizure activity check was performed after the detection of GPDs, since GPD patterns can also have an increased amplitude, synchronization and periodicity. Two less specific features were the SEF and ADR. Although they are very sensitive for the detection of slowing, these features are only useful when other EEG abnormalities (such as seizure activity) are excluded. For this reason, the SEF and ADR values were placed at the bottom of the tree, to distinguish slowed EEG patterns from normal EEG registrations. Diagrams of the full decision tree are presented in Figs. 3 and 4.

Table 3
The most common EEG patterns and the quantitative EEG features used to classify these patterns. The features are listed in the same order as they appear in the decision tree.

EEG pattern	Quantitative EEG feature
Iso-electric	Mean amplitude
Low voltage	Mean amplitude
Artefacts	High to low frequency ratio, mean amplitude
Burst suppression	Burst and suppression index
GPDs	Burst and suppression index
Seizure activity	Autocorrelation, nearest neighbor synchronization, mean amplitude
Slowing	Spectral edge frequency and alpha to delta ratio
Normal	–

2.4. User interface

The output of the decision tree is displayed in a novel user interface. The user interface of two epochs of the test set are shown together with a small part of the raw EEG in Fig. 5. The upper left part of the interface consists of four plots, one for each brain region, with the output of the decision tree as a function of the epoch number. In the two upper figures on the right side, the trend of the BSI and the power spectrum of both hemispheres are shown. Since asymmetries can only be measured when the activity of left and right hemispheres are compared, the BSI cannot be calculated for each brain region separately and is therefore displayed separately. In the bottom part of the interface, the interpretation of the preceding 5 min recording is presented in a textbox for each brain region separately. This interpretation is equal to the most prevalent output of the decision tree for each brain region in this

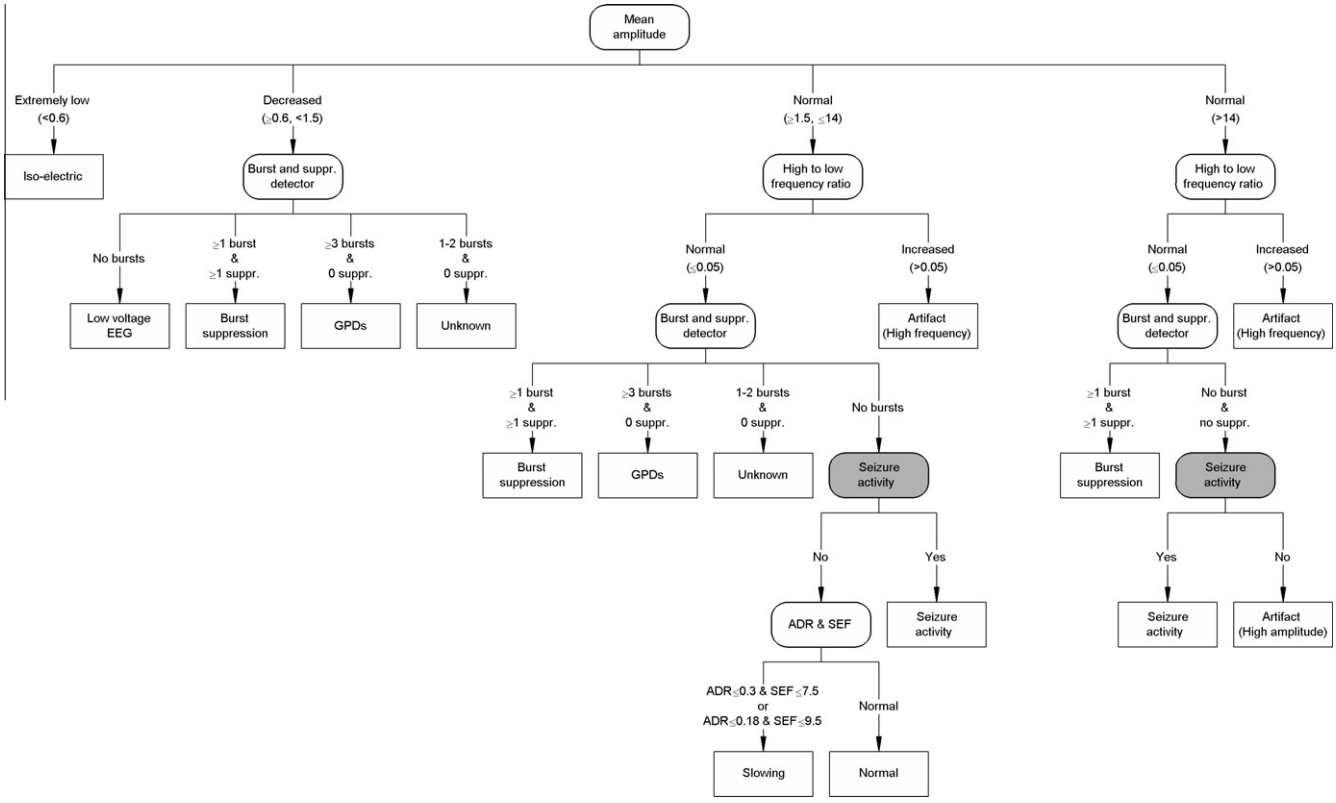

Fig. 3. Structure of the decision tree for the classification of the EEG per 10 s epoch and per brain region (left anterior, left posterior, right anterior, right posterior). In this figure, the gray colored 'Seizure Activity Tree' blocks represent a smaller decision tree (Fig. 4). ECG artefacts can increase the mean amplitude of an iso-electric EEG significantly. Therefore, the boundary for the mean amplitude between 'extremely low' and 'decreased' is increased to 1 μV in EEG signals with a high correlation to the ECG signal. All other boundaries in the decision tree are fixed. ADR = alpha to delta ratio, SEF = spectral edge frequency.

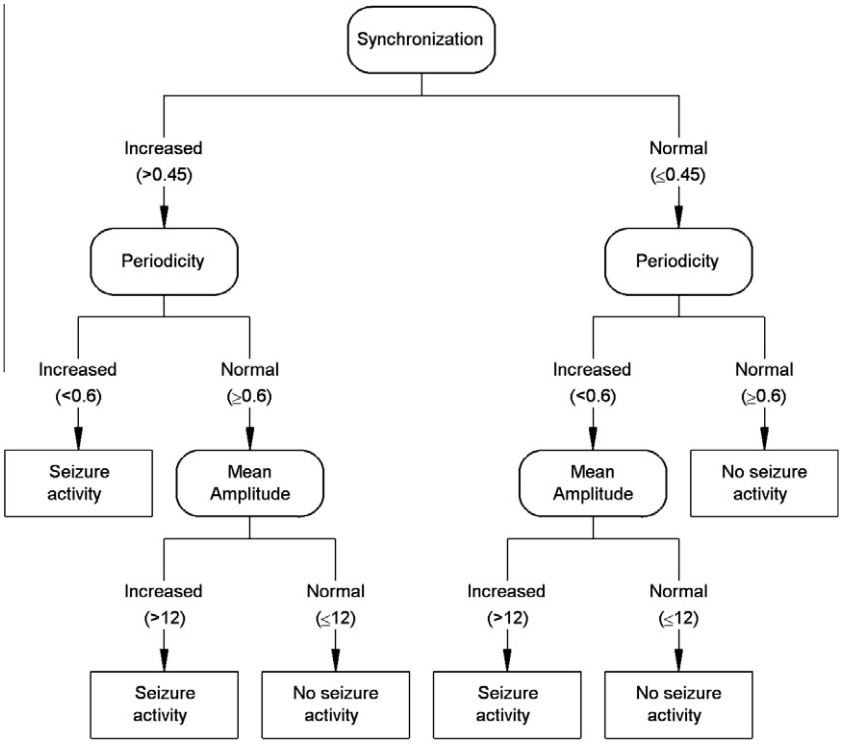

Fig. 4. Decision tree for the detection of seizure activity. This tree represents the gray colored 'Seizure Activity Tree' blocks in the overall decision tree of Fig. 3. This smaller decision tree is used to detect whether an epoch contains seizure activity, and its output is either 'No' (no seizure activity) or 'Yes' (seizure activity). This decision is made based on a combination of synchronicity, periodicity and mean amplitude of the EEG signal. After this decision, the remainder of the overall decision tree (Fig. 3) is used for the final categorization of the epoch.

time frame. Two exceptions are made for iso-electric EEGs and burst suppression patterns with long suppressions. To classify an EEG as iso-electric, all four brain regions have to be iso-electric for the complete 5 min. If not, the EEG is interpreted as low voltage. If most of the epochs were interpreted as iso-electric or low voltage, and a few as burst suppression, the EEG was interpreted as a burst suppression pattern with long interburst intervals.

In addition to these outputs, a range of possibilities was introduced for the interpretation of the BSI: EEGs were classified as 'symmetric', 'slightly asymmetric' or 'asymmetric'. In a diffuse slowed EEG, the degree of diffuse slowing ('severe slowing', 'slowing' or 'moderately slowing') was displayed as well. Finally, the computer interpretation of the last 5 min was illustrated using a color coded head. This head displays a brain region as red for seizure activity or GPDs, gray for normal EEGs, blue for slowing, burst suppression or low voltage EEGs, or black for iso-electric EEGs.

2.5. Implementation for real-time analysis

Our interpretation algorithms were implemented into the Neurocenter EEG monitoring system of the Medisch Spectrum Twente (Neurocenter EEG, Clinical Science Systems, Netherlands). Instead of using Matlab, the scripts were executed in the GNU Octave open source platform (http://www.octave.org).

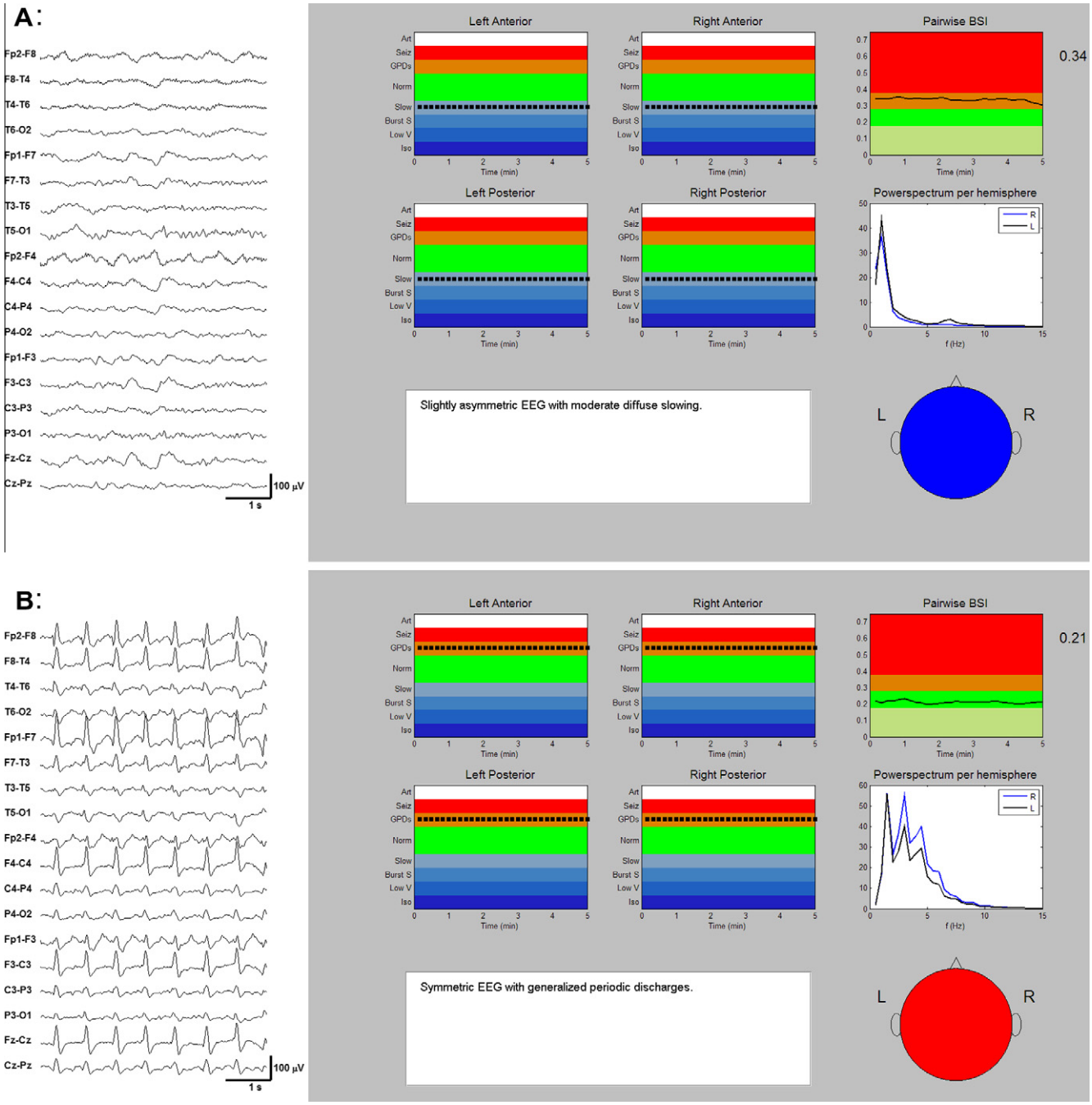

Fig. 5. Two examples of the user interface showing the results for two registrations of the test set, together with a small part of the raw EEG. The results of the decision tree are displayed in the interface as trend curves (upper panels) and in text (lower left panel). (ART = artefact, seiz = seizure activity, GPDs = generalized periodic discharges, norm = normal, slow = slowing, burst S = burst suppression, low V = low voltage, iso = iso-electric and BSI = Brain Symmetry Index). A: User interface of a neurotrauma patient with diffuse slowing (patient # 14). B: User interface of an EEG epoch containing GPDs (patient # 18).

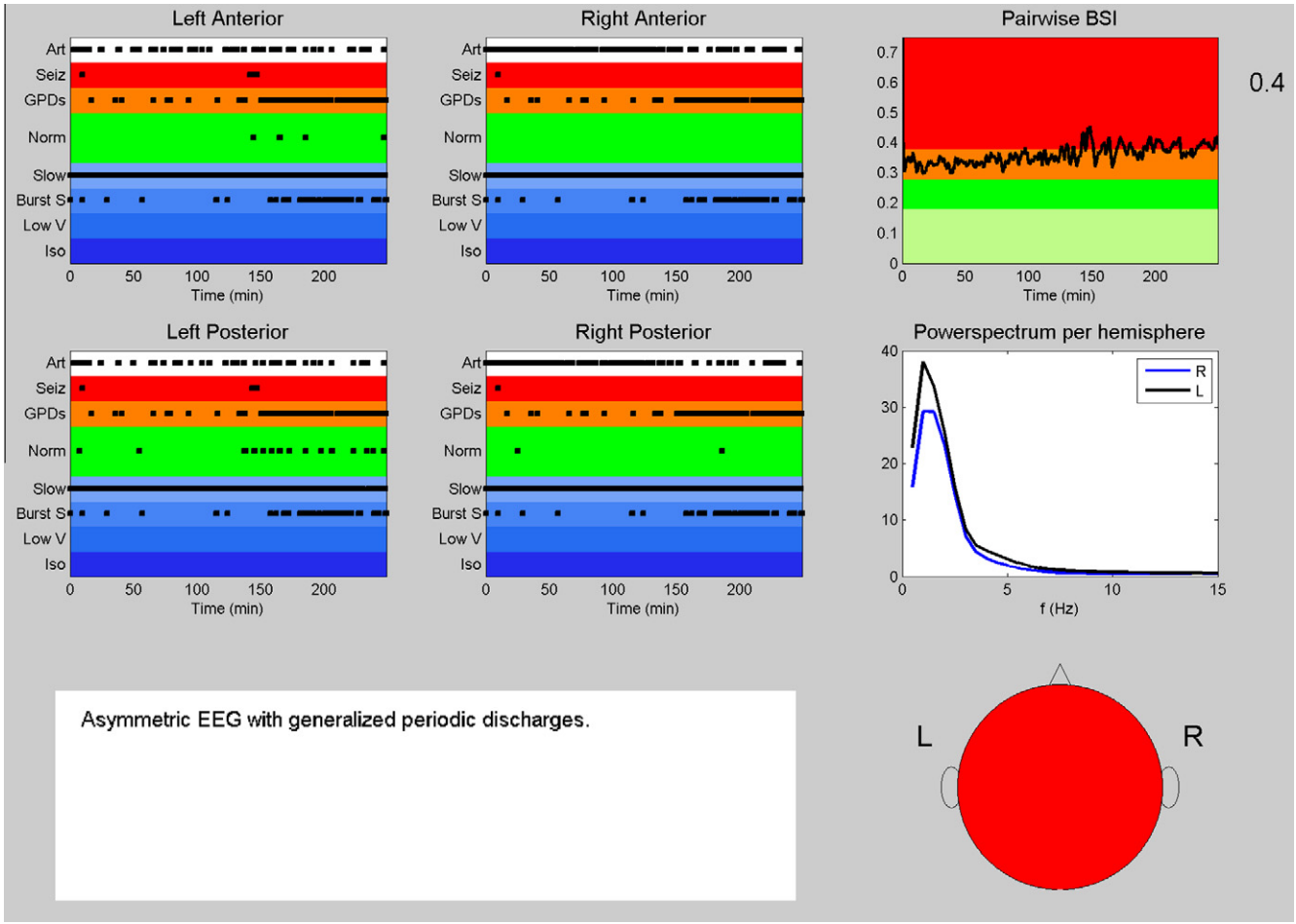

Fig. 6. The user interface of a long EEG registration (>4 h) for patient #1. Initially, the EEG shows a diffuse slowed pattern with many EMG artefacts. After a few hours it evolves into GPDs and an occasional burst suppression pattern. The conclusion (represented as the color coded map and in text) is based on the preceding 5 min of EEG. (ART = artefact, seiz = seizure activity, GPDs = generalized periodic discharges, norm = normal, slow = slowing, burst S = burst suppression, low V = low voltage, iso = isoelectric and BSI = Brain Symmetry Index).

3. Results

The results obtained from evaluating the training set with the final version of the decision tree are given in Table 1. In the training set, 36 out of 41 EEGs (88%) were classified correctly. Two out of the five misclassifications can be explained by artefacts. One of them was an EEG with a burst suppression pattern. The suppressions were not detected due to artefacts in the signal, although a correct warning about the presence of artefacts was given. In the other EEG, artefacts were wrongly interpreted as seizure activity instead of high amplitude artefacts. Two other misclassifications were caused by either missing bursts or GPDs with low amplitudes. The final EEG was misclassified in a single brain region, where slowing of the EEG was classified as seizure activity, the other three brain regions were classified correctly as slowing.

After optimizing the decision tree with the training set, an evaluation was done on a new independent test set. The outcome of this evaluation is shown in Table 2. Seventeen out of 20 EEGs (85%) were classified correctly. Of the three incorrect interpreted EEGs, two were low voltage EEGs. One of the low voltage EEGs contained many ECG artefacts and these were interpreted as bursts. This caused the EEG to be misclassified as a burst suppression pattern. The second low voltage EEG was classified as normal. The last misclassified EEG was caused by missing GPDs with low amplitude.

The real-time implementation of our system was evaluated in four ICU patients. Simulations in a Matlab environment showed that the algorithm was fast enough for real-time implementation; however the Octave implementation of Neurocenter was much slower. In fact, the current Octave version of the classifier allowed analysis of only the first 10 s of each 30 s in real-time, while the other 20 s had to be discarded. The raw EEG data was stored without interruption to be available for review by the consulting neurologist. No other technical problems occurred during the measurements. For each of the four registrations, the classifier showed satisfying correspondence between our system and human interpretation. An example of the interface in a long term (4 h) registration is shown in Fig. 6. At the beginning of the registration, the EEG was mainly diffuse slowed with superimposed muscle contraction artefacts. At the end of the EEG, the pattern showed GPDs and periods of burst suppression which was interpreted correctly by the classification algorithm. In this particular case, this was initially noted by the interpretation of the user interface. Subsequent reviewing of the raw EEG data indeed showed GPDs. The patient was treated for a non-convulsive status epilepticus and recovered well.

4. Discussion

Monitoring brain function in the ICU is very important, since ICU patients are at high risk of various secondary brain injuries

such as seizures or cerebral ischemia. Although the EEG is very sensitive in detecting changes in the neurological status of patients, cEEG monitoring in the ICU is limited due to the fact that the signals are difficult to interpret by non-experts. A reliable real-time classification system will reduce the drawback of the visual interpretation burden and will facilitate the use of cEEG in the ICU. This should allow earlier diagnosis of ischemic events and seizure activity. With the current availability of treatments for acute ischemia, the early detection of cerebral ischemia (in a reversible state) has great potential for infarct prevention (Hirsch and Kull, 2004). Seizures after brain injury are associated with a less favorable clinical outcome (Vespa, 2005; Oddo et al., 2009), and early detection and treatment can most likely improve the outcome. Early detection of seizures with cEEG is therefore very relevant to protect the brain from seizure-related injury in critically ill patients (Claassen et al., 2004b; Vespa, 2005).

In this study, we present an EEG classification system for monitoring ICU patients, based on a combination of eight qEEG features. Thirty-six EEG epochs out of 41 (88%) and 17 epochs out of twenty (85%) were classified correctly in the training and test set respectively. These results indicate that the system can have a significant impact in the clinical setting. For example, the group of slowed EEGs was classified very well, showing that early detection and treatment of ischemic events is possible. Although our algorithms do not yet reach the classification accuracy of an experienced electroencephalographer, it does allow for an initial evaluation by non-EEG experts and facilitates the use of cEEG monitoring in the ICU. A regular review of the EEG data by electroencephalograhpers remains of course an essential part in the decision making process.

The two low voltage, but otherwise normal EEGs included in the test set were both misclassified, most likely because of insufficient training the decision tree on low voltage EEGs: only one low voltage EEG was included in the training set. Because of this, the chosen boundary for the mean amplitude between normal and low-voltage might have been chosen too low. In one of the misclassified low voltage EEGs, many ECG artefacts were interpreted as bursts and this was misclassified as a burst suppression pattern. The second low voltage (but normal) EEG was classified as normal; therefore the misclassification would have had minimal clinical impact. Although great care was taken to select artefact-free epochs, various registrations included in the test set did contain artefacts. Most of the misclassifications were caused by the presence of these artefacts or by missing low amplitude bursts or GPDs. We tried to train the system in handling EEGs with artefacts by including three registrations with artefacts in the training set. However, we are well aware that the number of different artefacts is much larger than three and that the present system is not sufficiently trained for all artefact types. As the reliable detection of artefacts is highly relevant in the daily use of a system in the ICU, additional improvements for the detection of artefacts are required.

It is well known that critically ill patients with GPDs have a poor prognosis for survival, but at present it is not clear if treating or preventing GPDs will lead to an improved outcome in these patients (Chong and Hirsch, 2005; Claassen et al., 2007; Oddo et al., 2009; San-Juan et al., 2009). There is no consensus regarding the need to treat GPDs or how aggressively they should be treated (Hirsch et al., 2005). Therefore, the clinical consequences of missing GPDs by the classifier are unclear.

A novel interface for our classification system was presented. The text output and color coded head in the interface allow a quick interpretation by non-EEG experts. Extra panels in the interface present additional information to the neurologist and clinical neurophysiologist, and the raw EEG data can still be reviewed by the consulting neurologist or clinical neurophysiologist. The dynamics of longer EEG registrations can be seen with a single glance at the four time-curves representing the output of the decision tree for each of the four brain regions.

In the comparison with the clinical evaluation, we used the output of the classifier. Therefore, there was no additional visual interpretation of the trend curves in the user interface. Of course, it is possible that the EEG shows significant changes within 5 min which may limit the performance of the classifier. Therefore, for our present evaluation we decided to use uniform EEG epochs.

The system was implemented in a dedicated EEG monitor suitable for real-time analysis in the ICU. Pilot measurements performed in four neurological ICU patients showed that the real-time use of the classification system at the bedside of the patient is technically feasible. However, we note that the current real-time implementation of the classifier allowed analysis of the first 10 s of each 30 s epoch only, while the other 20 s had to be discarded for computational reasons. With more efficient routines, faster software, and higher processing speeds, skipping epochs should not be necessary. Given the typical time scales during which changes occur however, this does not seem to be a critical issue. The evaluation of our system in four real-time registrations was satisfying. Our first impression was that the performance in these registrations was similar to those obtained in the offline analysis. An extended evaluation in a larger group of ICU patients is currently in progress.

Similar to the observations presented in the study of Claassen et al. (2004b), recordings in our patients showed that continuous monitoring is highly relevant to reliably detect seizure activity. The use of cEEG registrations and computer interpretation had an impact on the clinical decision making in all four of the patients who were monitored in the ICU.

The classification accuracy of the test set and the results of the real-time pilot measurements are encouraging, but it is clear that an evaluation on a larger group of EEGs is needed for additional testing and improvements. The addition of an alarm mechanism to the real-time monitor may also further improve the clinical impact of the system. Integration with other clinical measures such as blood pressure, temperature, intracranial pressure (Jordan, 1995), near-infrared spectroscopy (Calderon-Arnulphi et al., 2007), drug intake and video (Hirsch and Kull, 2004; Kull and Emerson, 2005) can further contribute to improved brain monitoring in the ICU, ultimately resulting in the realization of a multidimensional monitoring system (Wartenberg and Mayer, 2005).

The main focus of our study was to explore whether computer assisted EEG diagnostics can assist in the visual interpretation by experienced electroencephalographers. We did not evaluate the reproducibility of the EEG classification, although this is an important issue. Since the system has been trained by labeled EEG data from the same department, it cannot excluded that there is a particular bias in the classification. Therefore, training and evaluating the system using a larger dataset of different centres may improve the performance of the classifier.

In closing, we remark that most existing real-time EEG systems focus on the detection of seizures or one specific EEG pattern. Particularly in neonates, several automatic seizure detection systems have been proposed (Liu et al., 1992; Gotman et al., 1997; Celka and Colditz, 2002; Aarabi et al., 2006; Deburchgraeve et al., 2008). However, the EEG in neonates is not comparable to the EEG in adult patients. What makes our system unique is that the classification of most common EEG patterns encountered in the adult ICU is combined into one system. In addition, the classifier is patient independent and no patient specific boundaries or parameters have to be set.

In conclusion, we present a decision tree using eight qEEG features to classify the most common EEG patterns in the adult neurological ICU. This allows us to differentiate between the most

common EEG patterns: normal, iso-electric, low voltage, burst suppression, focal or diffuse slowing, GPDs and seizure activity. At present, we achieve a satisfying classification accuracy of 85%. The monitoring system allows real-time classification and subsequent interpretation by ICU personnel. Ultimately, this can contribute to an increased use of real-time EEG monitoring in ICU patients, thereby allowing early detection of neurological derangements and introducing the potential for early interventions.

Acknowledgements

T. Heida Ph.D., A. de Keijzer Ph.D. and the ICU staff and personnel of the Medisch Spectrum Twente, Enschede, The Netherlands, are acknowledged for the fruitful discussions during the preparation of this paper. S.S. Lodder M.Sc. is acknowledged for the critical reading of the manuscript. Michel van Putten is co-founder and medical advisor of Clinical Science Systems, the Netherlands. The remaining authors have not disclosed any potential conflicts of interest.

References

Aarabi A, Wallois F, Grebe R. Automated neonatal seizure detection: a multistage classification system through feature selection based on relevance and redundancy analysis. Clin Neurophysiol 2006;117:328–40.

Calderon-Arnulphi M, Alaraj A, Amin-Hanjani S, Mantulin WW, Polzonetti CM, Gratton E, et al. Detection of cerebral ischemia in neurovascular surgery using quantitative frequency-domain near-infrared spectroscopy. J Neurosurg 2007;106:283–90.

Celka P, Colditz P. A computer-aided detection of EEG seizures in infants: a singular-spectrum approach and performance comparison. IEEE Trans Biomed Eng 2002;49:455–62.

Claassen J, Hirsh L, Kreiter KT, Du EY, Connolly ES, Emerson RG, et al. Quantitative continuous EEG for detecting delayed cerebral ischemia in patients with poor-grade subarachnoid haemorrhage. Clin Neurophysiol 2004a;115:2699–710.

Claassen J, Mayer SA, Kowalski RG. Detection of electrographic seizures with continuous EEG monitoring in critically ill patients. Neurology 2004b;62: 1743–8.

Claassen J, Mayer SA, Hirsch LJ. Continuous EEG monitoring in patients with subarachnoid hemorrhage. J Clin Neurophysiol 2005;22:92–8.

Claassen J, Jetté N, Chum F, Green R, Schmidt M, Choi H, et al. Electrographic seizures and periodic discharges after intracerebral hemorrhage. Neurology 2007;69:1356–65.

Chong DJ, Hirsch LJ. Which EEG patterns warrant treatment in the critically ill? Reviewing the evidence for treatment of periodic epileptiform discharges and related patterns. J Clin Neurophysiol 2005;22:79–91.

Deburchgraeve W, Cherian PJ, de Vos M, Swarte RM, Blok JH, Visser GH, et al. Automated neonatal seizure detection mimicking a human observer reading EEG. Clin Neurophysiol 2008;119:2447–54.

Finnigan SP, Rose SE, Walsch M, Griffin M, Janke AL, McMahon KL, et al. Correlation of quantitative EEG in acute ischemic stroke with 30-day NIHSS score. Comparison with diffusion and perfusion MRI. Stroke 2004;35:899–903.

Finnigan SP, Walsh M, Rose SE, Chalk JB. Quantitative EEG indices of sub-acute ischaemic stroke correlate with clinical outcomes. Clin Neurophysiol 2007;118:2525–32.

Friedman D, Claassen J, Hirsch LJ. Continuous electroencephalogram monitoring in the intensive care unit. Anesth Analg 2009;109:506–23.

Gotman J, Flanagan D, Rosenblatt B, Bye A, Mizrahi EM. Evaluation of an automatic seizure detection method for the newborn EEG. Electroencephalogr Clin Neurophysiol 1997;103:363–9.

Hirsch LJ, Kull LL. Continuous EEG monitoring in the intensive care unit. Am J of Electroneurodiagnostic Technol 2004;44:137–58.

Hirsch LJ, Brenner RP, Drislane FW, So E, Kaplan PW, Jordan KG, et al. The ACNS subcommittee on research terminology for continuous EEG monitoring: proposed standardized terminology for rhythmic and periodic EEG patterns encountered in critically ill patients. J Clin Neurophysiol 2005;22:128–35.

Jordan KG. Neurophysiologic monitoring in the neuroscience intensive care unit. Neurol Clin 1995;13:579–626.

Jordan KG. Continuous EEG monitoring in the neuroscience intensive care unit and emergency department. J Clin Neurophysiol 1999;16:14–39.

Jordan KG. Emergency EEG and continuous EEG monitoring in acute ischemic stroke. J Clin Neurophysiol 2004;21:341–9.

Kull LL, Emerson RG. Continuous EEG monitoring in the intensive care unit: technical and staffing considerations. J Clin Neurophysiol 2005;22:107–18.

Leon-Carrion J, Martin-Rodriguez JF, Damas-Lopez J, Barroso y Martin JM, Dominguez-Morales MR. Delta–alpha ratio correlates with level of recovery after neurorehabilitation in patients with acquired brain injury. Clin Neurophysiol 2009;120:1039–45.

Jia X, Koenig MA, Nickl R, Zhen G, Thakor NV, Geocadin RG. Early electrophysiologic markers predict functional outcome associated with temperature manipulation after cardiac arrest in rats. Crit Care Med 2008;36:1909–16.

Liu A, Hahn JS, Heldt GP, Coen RW. Detection of neonatal seizures through computerized EEG analysis. Electroencephalogr Clin Neurophysiol 1992;82:30–7.

Oddo M, Carrera E, Claassen J, Mayer SA, Hirsch LJ. Continuous electroencephalography in the medical intensive care unit. Crit Care Med 2009;37:2051–6.

Russell SJ, Norvig P. Artificial intelligence. A modern approach. 1st ed. Upper Saddle River: Prentice-Hall; 1995.

San-Juan OD, Chiappa KH, Costello DJ, Cole AJ. Periodic epileptiform discharges in hypoxic encephalopathy: BiPLEDs and GPEDs as a poor prognosis for survival. Seizure 2009;18:365–8.

Scheuer ML. Continuous EEG monitoring in the intensive care unit. Epilepsia 2002;43:114–27.

Sheorajpanday RVA, Nagels G, Weeren AJT, van Putten MJAM, De Deyn PP. Reproducibility and clinical relevance of quantitative EEG parameters in cerebral ischemia: a basic approach. Clin Neurophysiol 2009;120:845–55.

Slooter AJC, Vriens EM, Leijten FSS, Spijkstra JJ, Girbes ARJ, van Huffelen AC, et al. Seizure detection in adult ICU patients based on changes in EEG synchronization likelihood. Neurocrit Care 2006;3:186–92.

Tonner PH, Bein B. Classic electroencephalographic parameters: median frequency, spectral edge frequency, etc.. Best Pract Res Clin Anaesthesiol 2006;20:147–59.

Tempelhoff R, Yoder J. Monitoring the brain: lack of tools or lack of will? Crit Care Med 2008;36:1983–4.

van Putten MJAM, Tavy DLJ. Continuous quantitative EEG monitoring in hemispheric stroke patients using the brain symmetry index. Stroke 2004;35:2489–92.

van Putten MJAM, Kind T, Visser F, Lagerburg V. Detecting temporal lobe seizures from scalp EEG recordings: a comparison of various features. Clin Neurophysiol 2005;116:2480–9.

van Putten MJAM. The colorful brain: visualization of EEG background patterns. J Clin Neurophysiol 2005;25:63–8.

van Putten MJAM. Extended BSI for continuous EEG monitoring in carotid endarterectomy. Extended BSI. Clin Neurophysiol 2006;117:2661–6.

van Putten MJAM. The revised brain symmetry index. Clin Neurophysiol 2007;118:2362–7.

Vespa PM, Nuwer MR, Juhász C, Alexander M, Nenov V, Martin N, et al. Early detection of vasospasm after acute subarachnoid hemorrhage using continuous EEG ICU monitoring. Electroencephalogr Clin Neurophysiol 1997;103:607–15.

Vespa P. Continuous EEG monitoring for the detection of seizures in traumatic brain injury, infarction, and intracerebral hemorrhage: "to detect and protect". J Clin Neurophysiol 2005;22:99–106.

Wartenberg KE, Mayer SA. Multimodal brain monitoring in the neurological intensive care unit: where does continuous EEG fit in? J Clin Neurophysiol 2005;22:124–7.

Wennervirta JE, Ermes MJ, Tiainen SM, Salmi TK, Hynninen MS, Särkelä MO, et al. Hypothermia-treated cardiac arrest patients with good neurological outcome differ early in quantitative variables of EEG suppression and epileptiform activity. Crit Care Med 2009;37:2427–35.